Base-Pair Dynamics in an Antiparallel DNA Triplex Measured by Catalyzed Imino Proton Exchange Monitored via ^{1}H NMR Spectroscopy†

Sebastian Wärmländer,‡ Karin Sandström,‡ Mikael Leijon,§ and Astrid Gräslund*,‡

Department of Biochemistry and Biophysics, Arrhenius Laboratory, Stockholm University, S-106 91 Stockholm, Sweden, and LightUp Technologies AB, Lunastigen 5, S-141 44 Huddinge, Sweden

Received March 24, 2003; Revised Manuscript Received July 7, 2003

ABSTRACT: Using ^{1}H NMR spectroscopy, the base-pair opening dynamics of an antiparallel foldback DNA triplex and the corresponding duplex has been characterized via catalyzed imino proton exchange. The triplex system was found to be in an equilibrium between a duplex and a triplex form. The exchange rate between the two forms (i.e., the on/off-rate of the third strand) was measured to be 5 s^{-1} at 1 °C, and the base-pair dynamics of both forms were investigated separately. Both Watson−Crick and reverse Hoogsteen base pairs were found to have base-pair lifetimes in the order of milliseconds. The stability of the Watson−Crick base pairs was, however, substantially increased in the presence of the third strand. In the DNA triplex, the opening dynamics of the reverse Hoogsteen base pairs was significantly faster than the dynamics of the Watson−Crick pairs. We were able to conclude that, for both Watson−Crick and reverse Hoogsteen base pairs, spontaneous and individual opening from within the closed base triplet is the dominating opening pathway.

The base-pair opening dynamics in DNA has been the subject of numerous studies since base-pair opening is implicated in a number of important cellular processes such as transcription and recombination. Previous work has established that within duplex DNA base pairs open individually and spontaneously and that base-pair opening is sensitive to structural perturbations (*1*, *2*). Base-pair opening dynamics of triple-helical DNA is, however, less well-investigated.

DNA triple helices form when a third strand binds in the major groove of a homopurine/homopyrimidine DNA duplex (*3*). Triple helices have generated considerable interest since their existence in vivo has led to speculation and research into possible biological roles for this structural motif (*4*). In addition, triple-helix DNA forms the basis for the anti-gene strategy of controlling gene expression, where a short third strand is used as a therapeutic agent to block the transcription of a specific gene (*5*, *6*).

Pyrimidine rich third strands bind parallel to the duplex purine strand through Hoogsteen bonds, forming the isosteric canonical triplets T−A·T and C−G·C^+ ("−" and "·" denotes Watson−Crick and Hoogsteen pairing, respectively), where the protonation of the third-strand cytosines makes the stability of these systems pH-dependent. Purine rich third strands, on the other hand, bind antiparallel to the duplex purine strand through reverse Hoogsteen bonds, forming the pH-insensitive and nonisosteric canonical triplets G·G−C and A·A−T. Also, T·A−T triplets may be incorporated in antiparallel triplexes through reverse Hoogsteen bonds. The affinity and specificity of third-strand binding is affected by a number of factors such as sequence length and composition, the presence of base-pair mismatches, and solution conditions, including pH and mono- and divalent counterion concentrations (*3*).

The static 3-D structures of parallel triplexes are relatively well-known from a number of crystallographic and NMR studies. Antiparallel triplexes, although less investigated, seem to have similar overall structural properties as parallel triplexes despite the nonisosteric base triplets (*6*).

The dynamic properties of triplex DNA are less well-known. Such information is important for understanding the factors that stabilize both Watson−Crick and non-Watson−Crick DNA structures and may be helpful in understanding the possible biological role of DNA triplexes, as well as aiding in the design of oligonucleotides for binding duplexes both in vitro and in vivo. Previously, it has been shown that the imino proton exchange rates of Watson−Crick base pairs in parallel DNA triplexes are significantly reduced in the presence of a third strand (*7*, *8*).

In the present study, we have for the first time measured the base-pair dynamics for reverse Hoogsteen base pairs in a nativelike antiparallel DNA triplex. Furthermore, we present a comparison of the lifetimes and apparent dissociation constants of DNA Watson−Crick base pairs with and without a third strand being present in the major groove.

MATERIALS AND METHODS

Sample Preparations and Titrations. Two DNA systems were investigated, an antiparallel foldback triplex system (DNA-1) and the corresponding foldback duplex (DNA-2) (Figure 1).

The oligonucleotides were purified on NAP-10 Columns (Pharmacia Biotech) and dissolved in a 3 mM borate buffer

† This study was supported by grants from The Swedish Research Council.

* Corresponding author. E-mail: astrid@dbb.su.se. Tel: 46-8-162450. Fax: 46-8-155597.

‡ Stockholm University.

§ LightUp Technologies AB.

10.1021/bi034479u CCC: $25.00
Published on Web 10/10/2003

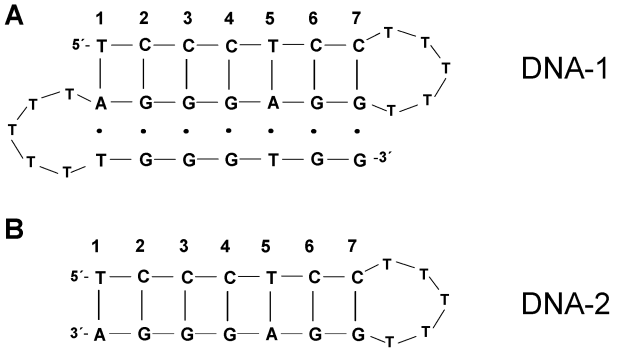

FIGURE 1: Investigated DNA systems: the antiparallel foldback triplex system (DNA-1) (A) and the corresponding foldback duplex (DNA-2) (B). Watson−Crick base pairs are represented with dashes (−), and Hoogsteen base pairs are represented with dots (·).

(90% H_2O and 10% D_2O) containing 100 mM NaCl and adjusted to pH 8.8. The duplex and triplex concentrations were in the range of 0.2−2 mM. Base catalyst titrations were carried out at 1 and 15 °C for the duplex and at 1 °C for the triplex with a 6.3 M ammonia buffer adjusted to pH 8.8. The pH of the buffer was measured with a double-junction high-salt Orion 8103 Ross electrode, and the [acid]/[base] fractions of the buffer were obtained from the amounts of salt and liquid base used to prepare the buffer.

NMR Spectroscopy. All NMR[1] experiments were carried out on a Varian Inova 600 MHz spectrometer.

Imino Proton Resonance Assignments. The resonance assignments of the imino protons, in duplex as well as in triplex, were obtained from NOESY experiments, conducted with a mixing time of 250 ms at 1 °C. A jump−return observe pulse was used to avoid excitation of the water resonance (*9*). Linear prediction was employed in the indirect dimension to increase resolution. All 2-D data processing was carried out with Felix97 (Molecular Simulations Inc.).

Imino Proton Exchange Measurements. The imino proton exchange times, τ_{ex}, at different catalyst concentrations, were obtained from measurements of the inversion recovery times in the presence, T_{rec}, and in absence, T_{aac}, of exchange catalyst according to

$$\frac{1}{\tau_{ex}} = \frac{1}{T_{rec}} - \frac{1}{T_{aac}} \tag{1}$$

Apart from longitudinal dipolar relaxation, direct exchange to water as well as exchange catalyzed both by OH^- ions and acceptor nitrogen of the opposite base (*10*) contributes to the recovery rate of the imino protons in the absence of added catalyst ($1/T_{aac}$). However, these contributions remain constant when the catalyst is added and will be canceled in eq 1. Consequently, the exchange time τ_{ex} represents exchange via the added catalyst only. The inversion recovery experiment utilized a 1−1.4 ms iBURP pulse for selective inversion (*11*) and a 0.7−1 ms Gaussian observe pulse for selective detection (*12*). Right shift and linear prediction of the FID were employed to correct for magnetization evolution during the observed pulse. In addition to the inversion−recovery technique, magnetization transfer experiments also may be utilized to measure imino proton exchange rates. Recent studies have shown that the two methods give very similar results (*13*, *14*). In the present study, we have utilized the inversion−recovery method since it is fast and reliable, particularly for relatively short exchange times.

Base-Pair Dynamics and Imino Proton Exchange Theory. The connection between base pair opening and imino proton exchange is based on the assumption that exchange of the imino proton only occurs when the hydrogen bond to the acceptor of the complementary base in the base pair is shifted to some other proton acceptor present in the solvent (i.e., the base pair has opened (*15*)). Several exchange mechanisms are possible. Direct exchange to water or exchange catalyzed by the complementary base always occurs, although rather inefficiently due to the low pK_a of these acceptors. By addition of a catalyst with a higher pK_a (e.g., ammonia), near opening-limited exchange can be reached. For a base pair with multiple (n) open states, formed with rates k_{op}^n and closed with rates k_{cl}^n, and provided that $\sum_n k_{op}^n \ll k_{cl}^1, k_{cl}^2, ..., k_{cl}^m$, the total imino proton exchange rate k_{ex} equals the sum of the exchange rate from each opening mode (*14*)

$$k_{ex} = \sum_{n=1}^{m} \frac{k_{op}^n k_{tr}^i [B]}{k_{cl}^n/\alpha^n + k_{tr}^i [B]} \tag{2}$$

where α^n is a parameter taking into account the different accessibility of the imino proton in the open states and in the mononucleoside, and k_{tr}^i is the imino proton-transfer rate from the mononucleoside per mole of added base catalyst, which is related to the molar collision rate k_{coll} and the pK_a difference between the imino proton and the catalyst ($\Delta pK = pK_{a,i} - pK_{a,B}$) by (*16*)

$$k_{tr}^i = \frac{k_{coll}}{1 + 10^{\Delta pK}} \tag{3}$$

For a base pair with a single opening mode ($n = 1$) and with $k_{op} \ll k_{cl}$, eq 2 can be rewritten as

$$\tau_{ex} = \tau_{op} + \frac{1}{K_d \alpha k_{tr}^i [B]} \tag{4}$$

where τ_{ex} and τ_{op} are the inverse exchange and opening rates, respectively, and $K_d = k_{op}/k_{cl}$ is the base-pair dissociation constant. If eq 4 is valid, a plot of τ_{ex} versus 1/[B] yields a straight line where τ_{op} is obtained from the y-axis intercept and αK_d from the slope.

Dissociation of the Third Strand. The chemical exchange rate between the duplex and the triplex form of DNA-1 was obtained from a saturation transfer experiment. The transfer of saturation from a spin S to a spin I is in the ideal case described by the following (*17*):

$$S_z(\tau) = M_{S0}\left(\frac{k_{SI}}{\rho_S + k_{SI}} \exp[-\tau(\rho_S + k_{SI})] + \frac{\rho_S}{\rho_S + k_{SI}}\right) \tag{5}$$

where ρ_s is the relaxation rate of spin S, S_z is the time-dependent intensity of the resonance of spin S, M_{S0} is the equilibrium magnetization of spin S, and k_{SI} is the exchange rate between spins (states) S and I. The saturation-transfer

[1] Abbreviations: NMR, nuclear magnetic resonance; FID, free induction decay; NOESY, nuclear Overhauser effect spectroscopy.

Table 1: Base-Pair Lifetimes, τ_{op}, and Apparent Dissociation Constants, $\alpha \cdot K_{diss}$, for the Central Watson−Crick, WC, and Hoogsteen, HG, Base Pairs of DNA-1 and DNA-2[a]

τ_{op} (ms)

base pair	WC1	WC2	WC3	WC4	WC5	WC5*[b]	WC6	WC6*[b]	WC7
	A−T	G−C	G−C	G−C	A−T		G−C		G−C
DNA-2, 15 °C		<1		4 ± 2	<1		3 ± 1		
DNA-2, 1 °C		<1		17 ± 2	2 ± 1		5 ± 3		
DNA-1, 1 °C		19 ± 2			90 ± 4	4 ± 1	76 ± 10	5 ± 5	

base pair	HG1	HG2	HG3	HG4	HG5	HG6	HG7
	T−A	G−G	G−G	G−G	T−A	G−G	G−G
DNA-1, 1 °C		20[c] ± 2	15 ± 2		20[c] ± 2		

$\alpha K_{diss} \times 10^{-7}$

base pair	WC1	WC2	WC3	WC4	WC5	WC5*[b]	WC6	WC6*[b]	WC7
	A−T	G−C	G−C	G−C	A−T		G−C		G−C
DNA-2, 15 °C				13	260		20		
DNA-2, 1 °C				6	48		4		
DNA-1, 1 °C		8			8	60	3	7	

base pair	HG1	HG2	HG3	HG4	HG5	HG6	HG7
	T−A	G−G	G−G	G−G	T−A	G−G	G−G
DNA-1, 1 °C		22[c]	78		33[c]		

[a] The kinetic parameters were derived from from exchange data obtained from ammonia catalysis at pH 8.8 and fitted to eq 4. The errors were propagated from the standard deviations in the measured recovery times. [b] The base pairs marked with * represent Watson−Crick base pairs in the duplex form of DNA-1 (i.e., when the third strand has dissociated). [c] Because of spectral overlap, we were unable to unambiguously assign this resonance.

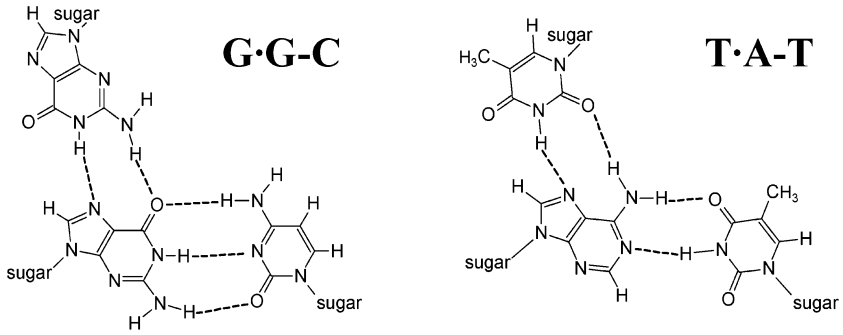

FIGURE 2: G·G−C and T·A−T base triplets.

experiment was achieved by low-power irradiation of the resonance of interest, during a variable time, immediately followed by a jump−return observe pulse (*9*).

RESULTS

Using ^{1}H NMR spectroscopy, the base-pair lifetimes and apparent dissociation constants of the antiparallel foldback triplex system DNA-1 and the corresponding hairpin duplex DNA-2 were characterized. The dynamical parameters were determined by measuring imino proton exchange times as a function of exchange catalyst concentration at 1 °C, pH 8.8 (Figure 4, Table 1). To facilitate comparisons with previous studies of DNA base-pair dynamics, the imino proton exchange of DNA-2 was also investigated at 15 °C. The base pairs of the two DNA systems investigated, DNA-1 and DNA-2, have been numbered as shown in Figure 1. Watson−Crick base pairs are represented with dashes (−), and Hoogsteen base pairs are represented with dots (·). Since each base pair, Watson−Crick as well as Hoogsteen, contains exactly one imino proton, the notation WC1 is used both to denote the Watson−Crick base pair number one and to denote the imino proton of this base pair (Figure 2).

Patel and co-workers have previously shown that DNA-1 forms an antiparallel triplex structure that is stable at low temperatures (*18*). Consequently, our exchange measurements were carried out at 1 °C. Although triplex systems have been shown to be substantially stabilized by Mg^{2+} ions, we have avoided using such ions, in order not to have divalent ions present when we titrate the sample with an ammonia buffer containing only monovalent ions.

Figure 3A,B shows the imino proton spectra of DNA-2 and DNA-1, respectively, at 1 °C. In the spectrum of DNA-1, resonances originating both from a triplex form and from a duplex form are present, and the resonances of the duplex form are indicated with a *. The imino proton resonances of both forms were assigned from NOESY experiments using the standard connectivity pathway (data not shown) (*19*). The triplex resonance assignment was in agreement with the results of Patel and co-workers (*18*). The resonances of the duplex form of DNA-1 have the same chemical shifts as the

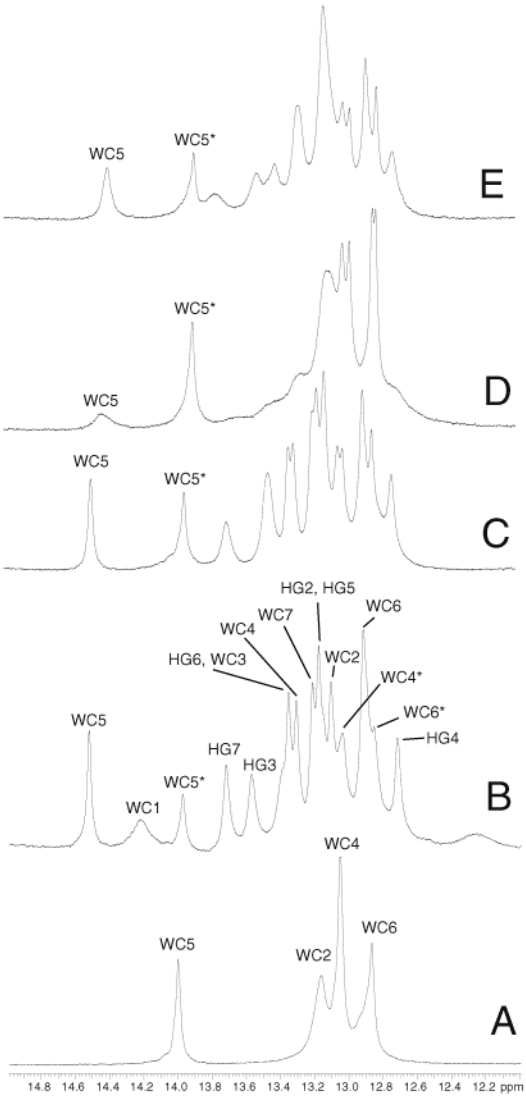

FIGURE 3: Imino proton spectra of DNA-2 at 1 °C (A) and of DNA-1 at 1 °C (B), 15 °C (C), 30 °C (D), and 30 °C after addition of 5 mM Mg^{2+} (E). The samples were dissolved in 100 mM NaCl buffer at pH 7.0. The base pairs marked with * represent Watson−Crick base pairs in the duplex form of DNA-1 (i.e., when the third strand has dissociated).

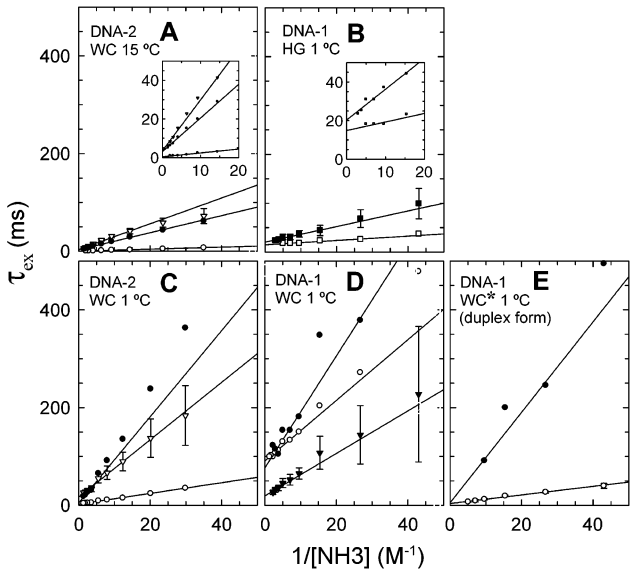

FIGURE 4: Imino proton exchange times vs inverse ammonia concentration, at pH 8.8. (A) Watson−Crick imino protons of DNA-2 at 15 °C. (B) Hoogsteen imino protons of DNA-1 at 1 °C. (C) Watson−Crick imino protons of DNA-2 at 1 °C. (D) Watson−Crick imino protons of DNA-1 in triplex form at 1 °C. (E) Watson−Crick imino protons of DNA-1 in duplex form at 1 °C. Open circle, WC5; filled circle, WC6; open triangle, WC4; filled triangle, WC2; open square, HG3; and filled square, HG2/HG5 (see text).

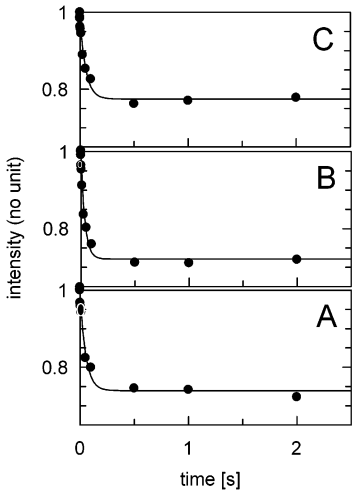

FIGURE 5: Saturation transfer data of DNA-1 at 1 °C (A), 30 °C (B), and 30 °C after addition of 5 mM Mg^{2+} (C). The samples were dissolved in 100 mM NaCl buffer at pH 7.0. The WC5 imino proton resonance of the triplex form of DNA-1 was selectively saturated for a variable time, and the intensity of the WC5* resonance of the duplex form of DNA-1 was subsequently measured. The vertical scale describes the intensity of WC5* as the fraction of equilibrium magnetization.

resonances of the hairpin DNA-2, indicating a similar structure (cf. Figure 3A,B).

Since antiparallel triplexes display no hypochromicity for the triplex to duplex transition, the triplex melting point cannot be obtained via UV spectroscopy. However, gradually increasing the temperature of the NMR sample, from 1 to 30 °C, shows that the triplex form of DNA-1 is present to a significant degree even at 30 °C, although the duplex form dominates at this temperature (Figure 3B−D). Adding 5 mM $MgCl_2$ to the sample at this temperature stabilizes the triplex form and shifts the equilibrium to more equal populations (Figure 3E). The results are consistent with previous studies where UV spectroscopy measurements indicated that antiparallel triplexes melt in a single 3 → 1 fashion (*20*, *21*), although the NMR results give a more detailed picture of the unfolding of the third strand as compared to the separation of the stem.

Dissociation of the Third Strand in the Triplex Sequence DNA-1. Under all experimental conditions, the imino proton spectra of DNA-1 show resonances originating both from the duplex and from the triplex form, indicating that the chemical exchange between the two forms is slow on the NMR time scale (Figure 3B−E). Since the WC5 imino proton has two well-resolved resonances, representing the duplex and triplex forms of DNA-1, it was possible to obtain the exchange rate between these two forms (i.e., the on/off-rate of the third strand) via saturation-transfer experiments. Thus, fitting the obtained data to eq 5 yielded on/off-rates of 4.9 s^{-1} at 1 °C and 7.6 s^{-1} at 30 °C (Figure 5). This weak temperature-dependence of the on/off-rate of the third strand

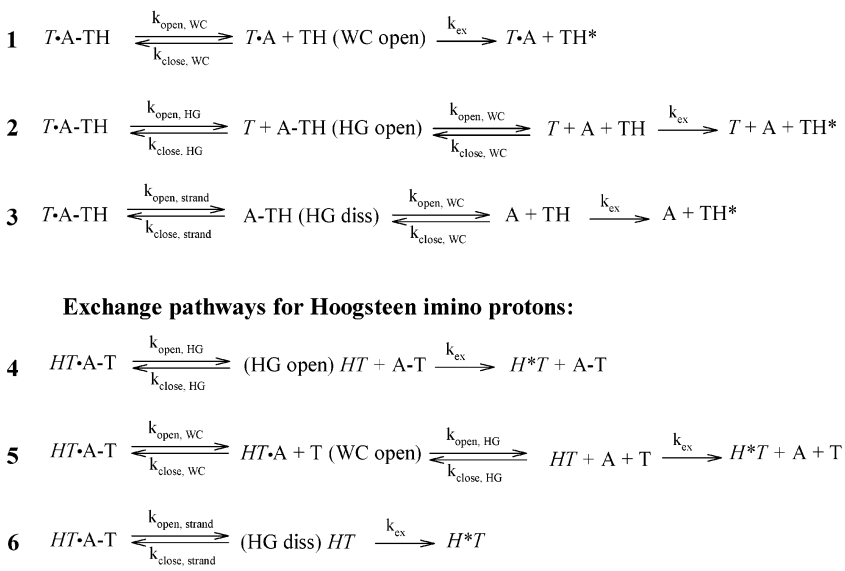

FIGURE 6: Possible imino proton exchange pathways. A T•A−T base triplet is taken as an example. Watson−Crick base pairs are represented with dashes (−), and Hoogsteen base pairs are represented with dots (•). The Hoogsten nucleotide is in italics. H denotes the exchangeable imino proton, and H* is the imino proton after exchange with the solvent protons.

is somewhat unexpected. Also, the stabilizing effect upon the third strand when 5 mM $MgCl_2$ is added to the sample is rather small, reducing the on/off-rate from 7.6 to 4.4 s^{-1} at 30 °C (Figure 5). Hence, we expect that also an increase of the ionic strength by additional ammonium ions has a similarly small effect on the stability of the third strand in the triplex.

Imino Proton Exchange. For T•A−T and G•G−C triplets, both the Watson−Crick and the Hoogsteen base pair contain imino protons (Figure 2). For these imino protons, there are a number of possible exchange pathways involving different open states. Some of these pathways are shown in Figure 6, where the Watson−Crick and Hoogsteen base pairs are assumed to open independently. It is possible that the Watson−Crick base pairs open directly from within the closed triplets (pathway 1), or they may open only after a Hoogsteen pair has opened (pathway 2). Naturally, they will also open when the Hoogsteen strand has dissociated (pathway 3). The Hoogsteen pairs may open individually within triplets (pathway 4) or only after a Watson−Crick pair previously has opened (pathway 5). A cooperative opening of the Hoogsteen pairs (i.e., dissociation of the third strand) will also lead to imino proton exchange (pathway 6). Pathways involving dissociation of the Watson−Crick strands are not included since this event occurs at a very low frequency.

For multistep mechanisms, such as pathways 3 and 5, the values of τ_{op} cannot be interpreted directly as individual rate constants, but the experimentally determined values of τ_{op} will nevertheless retain their meaning as the average lifetimes of the closed states. If exchange takes place from two or more pathways, then one pathway could dominate exchange at a low catalyst concentration and another could dominate at high catalyst concentration, leading to nonlinear exchange data according to eq 2. If, however, one pathway dominates the exchange at all catalyst concentrations, then eq 4 will apply, and the observed exchange data will be a linear function of the inverse catalyst concentration, 1/[B].

Base-Pair Opening Dynamics in the Hairpin Sequence DNA-2. WC Pairs. The imino proton spectrum of the duplex DNA-2 at 1 °C is shown in Figure 3A, and the exchange times of these imino protons are shown in Figure 4A,C at 15 and 1 °C, respectively. The most stable base pairs are found in the center of the sequence since end-fraying enhances the exchange of the outermost base pairs (Table 1). The thymine loop seems to stabilize the duplex since on the loop-end of the helix only the exchange of the outermost WC7 base pair is too fast to observe, while at the other end both WC1 and WC2 are significantly affected by end-fraying, and WC3 cannot be observed due to spectral overlap. As expected, all the central base pairs are stabilized when the temperature is decreased from 15 to 1 °C, and the G−C pairs, WC4 and WC6, are more stable than the A−T pair, WC5. The dynamics of the centermost WC4 pair is slightly faster than usual for a typical G−C pair at 15 °C (*1*), indicating that the 7-base-pair helix is somewhat unstable due to its short length.

Base-Pair Opening Dynamics in the Triplex Sequence DNA-1. WC Pairs. The imino proton spectra of the foldback triplex system DNA-1 at different temperatures are shown in Figure 3B−E. The exchange times of these imino protons at 1 °C are shown in Figure 4B,D,E, and the base-pair opening parameters derived from the exchange data are presented in Table 1. The results clearly show that the lifetimes of the Watson−Crick base pairs are increased dramatically in the presence of the third strand, from <1 to 19 ms for WC2, from 2 to 90 ms for WC5, and from 5 to 76 ms for WC6, at 1 °C. A corresponding decrease in the dissociation constant is also obvious. WC3 and WC4 cannot be observed due to spectral overlap, and WC1 and WC7 are lost due to end-fraying. The reason why WC6 is more stable than WC2 also in the triplex is probably because of the stabilizing effect of the thymine loop, which again reduces end-fraying.

Furthermore, it was possible to obtain exchange times (Figure 4E) for some of the Watson−Crick imino protons

of DNA-1 in duplex form (the resonances marked with a * in Figure 3B). By comparing the data sets of Figure 4E for the WC6* and WC5* imino protons with the corresponding data sets in Figure 4C for WC6 and WC5 in the DNA-2 duplex, it is evident that the exchange of these respective imino protons are identical, within the error limits. This shows that the exchange from the duplex form of DNA-1 is quite independent of the dissociation of the third strand, and no anomalies are seen in the linear exchange curves (Figure 4E).

The separate resonances of the duplex and triplex forms of DNA-1 allow us to discriminate between the opening pathway 3, where exchange from Watson−Crick imino protons takes place after dissociation of the third strand, and opening pathways 1 and 2, where exchange from Watson−Crick imino protons takes place in the presence of the third strand. Opening events from the duplex form, pathway 3, are monitored by measuring the *-resonances, whereas the other WC peaks are influenced by exchange from pathways 1 or 2. The fact that the exchange data is linear means that one of the pathways (1 or 2) dominates the other.

Base-Pair Opening Dynamics in the Triplex Sequence DNA-1. HG Pairs. Figure 4B shows the imino proton exchange data of HG3 and HG2/HG5. Only these Hoogsteen base pairs were monitored since the other resonances were lost either due to end-fraying or due to spectral overlap. One of the resonances was assigned to the HG3 pair and the other to either or both of the HG2 and the overlapping HG5 pairs. The HG2 pair is close to the end of the sequence and would be expected to be much-affected by end-fraying. However, the thymine loop of the third strand probably shields the HG2 pair from some of the end effects, and consequently, it is not possible to tell whether one or both of the HG2 and HG5 imino protons is being monitored.

The lifetimes of the two Hoogsteen base pairs were found to be 15 and 20 ms, and the apparent dissociation constants were 78 and $22/33 \times 10^{-7}$ (Table 1). The ambiguous 22/33 results from the uncertainty regarding whether the imino proton belongs to a thymine or a guanine since these bases have different intrinsic transfer rates for ammonia. After strand dissociation, the imino protons of the third strand are shifted to a region around 11 ppm (region not shown in Figure 3). Thus, the exchange following pathway (6), where exchange from third-strand imino protons takes place after the dissociation of the third strand, can be monitored independently from the exchange following pathways 4 and 5, where exchange from third-strand imino protons takes place from the intact triple helix. The exchange from the dissociated third strand (pathway 6) is, however, too fast to measure by the present methods, and the data reported are for either of the pathways, 4 or 5. Again, since the exchange data are linear, one of these pathways dominates the other.

DISCUSSION

Although the base-pair dynamics of DNA duplexes is rather well-characterized, much less is known about the base-pair dynamics of triplex systems. A few studies have been made on parallel pyr−pur−pyr triplexes, indicating that the opening fluctuations of the Watson−Crick base pairs are reduced when the third strand is added (*7*, *8*). However, parallel triplexes are only stable at acidic pH since the third-strand cytosines need to be protonated to form hydrogen bonds with the corresponding guanosine (*3*). High-accuracy measurements of base-pair dynamics, on the other hand, need to be carried out at alkaline pH in order for the base form of the exchange catalyst (e.g., ammonia) to reach sufficiently high concentrations. Cain and Glick addressed this problem by stabilizing the triplex with a disulfide cross-link and by using an exchange catalyst with a lower pK_a than ammonia (e.g., TRIS (*7*)). Although the lower pK_a of Tris allowed Cain and Glick to perform experiments at a close-to-neutral pH (i.e., 7.8), the low pK_a of Tris makes it a less effective proton-exchange catalyst, reducing the accuracy of the measurements.

For catalyst titration, one can in principle choose to keep the pH constant and vary buffer concentration or vary the pH while keeping the buffer concentration constant. In the present study, we have chosen the constant pH approach, as is the traditional way, and have also chosen it because our earlier studies indicate that evaluated base-pair lifetimes are pH-dependent (*14*).

In the present study, we present measurements of the base-pair dynamics for reverse Hoogsteen base pairs in a nativelike antiparallel DNA triplex. This triplex system is pH-insensitive, allowing us to perform the measurements at standard conditions (i.e., with ammonia at pH 8.8). As the third strand consists of guanines and thymines only, all bases in the third strand contain imino protons whose exchange can be monitored to yield information about the opening of the reverse Hoogsteen base pairs.

It has previously been shown that DNA base pairs in Watson−Crick duplexes open individually, with a lifetime of 1−10 ms for AT base pairs and 5−20 ms for GC base pairs at 15 °C (*1*). The base-pair dynamics of the duplex system DNA-2 at 15 °C conforms to this picture of shorter lifetimes for AT base pairs than for GC base pairs (Table 1). However, the lifetimes presented for DNA-2 in Table 1 are shorter than the typical values, probably due to end-fraying effects reaching into the short helix stem. Lowering the temperature to 1 °C slightly stabilizes the duplex hairpin: the base-pair lifetimes are somewhat increased, and end-fraying is reduced. It can be seen that the loop-end of the helix is the more stable end; probably this end is stabilized by a weak T−T base pair being present in the thymine loop.

The base-pair lifetimes of the Watson−Crick pairs are, however, dramatically increased when the third strand is present and bound (Table 1). This is consistent with the findings of Cain and Glick and of Russu and co-workers (*7*, *8*). The central Watson−Crick base pairs are stabilized by roughly a factor of 10, to 90 ms for the AT base pair WC5 and to 76 ms for the GC base pair WC3 (Table 1). The terminal base pairs are stabilized from <1 to ∼10 ms. Hence, the stabilizing effect of the third strand on the Watson−Crick base pairs extends over the whole sequence.

The slow exchange rate between the duplex and the triplex forms of DNA-1, approximately 5 s^{-1} at 1 °C and only weakly dependent on temperature, makes it possible to separately measure the base-pair dynamics of the duplex and triplex forms. Since the exchange rate between the duplex and the triplex forms of DNA-1 is in the same range as the imino proton exchange (at least at intermediate ammonia concentrations), it might be expected that the conformational

exchange of DNA-1 would affect the measured imino proton exchange rates. Indeed, dissociation of the third strand is an efficient pathway for exchange of the Hoogsteen imino protons. However, even in absence of added ammonia, at pH 8.8 the Hoogsteen imino protons exchange virtually every time the third strand dissociates, as evidenced by the extremely broad resonances of these protons (unpaired imino protons of the dissociated third strand exhibit resonances at around 11 ppm, data not shown). Hence, the proton exchange via this pathway is independent of the ammonia concentration and will consequently be canceled in eq 1. For the Watson−Crick imino protons, it is seen that the data obtained for DNA-1 in the duplex form correspond well to the data obtained for the hairpin DNA-2 alone (Table 1), providing further evidence for the transitions between the two forms of DNA-1 not affecting the measurements of the base-pair dynamics.

The dynamics of the triplex Hoogsteen base pairs is significantly faster than that of the corresponding Watson−Crick base pairs in the DNA-1 triplex form. The lifetime of, for example, HG3 (guanine) is 15 ms, considerably shorter than the 76 ms lifetime of the guanine WC6. The corresponding αK_d of HG3 is 78×10^{-7}, which is an order of magnitude larger than the corresponding αK_d values of the Watson−Crick base pairs in the triplex, again showing the faster dynamics of the Hoogsteen base pairs. Also, this finding is consistent with the results of Cain and Glick (*7*). The outermost base pairs of DNA-1 are not observable due to end-fraying, and similarly to DNA-2, also DNA-1 seems to be stabilized by the thymine loops, both regarding the Watson−Crick and the Hoogsteen base pairs.

These results now allow us to discriminate between the possible imino proton exchange pathways shown in Figure 6. Pathways 3 and 6 involve the initial dissociation of the third strand, which takes place on a time scale of seconds (see previously). The much faster observed opening of both the Watson−Crick and the Hoogsteen base pairs excludes these pathways. Thus, the different dissociation constants and lifetimes of the Hoogsteen base pairs show that these base pairs open and close spontaneously and individually, just like Watson−Crick base pairs. Furthermore, we can also discriminate between pathways 4 and 5. The linear appearance of the exchange data (Figure 4) shows that a single pathway dominates the imino proton exchange from the Hoogsteen base pairs. Since pathway 5 requires an initial opening of the WC base pair before an opening of the HG base pair, and since the opening dynamics of the HG base pairs is much faster than the dynamics of the WC base pairs, we conclude that the imino proton exchange of the Hoogsteen base pairs is dominated by pathway 4, where the Hoogsteen base pairs open from within the closed base triplet.

The exchange data for the Watson−Crick imino protons are linear, showing that a single pathway dominates also in this case (Figure 4). Since, in the triplex form, the opening rate of the Watson−Crick base pairs is slower than the opening rate of the Hoogsteen pairs, it is in principle possible that the opening of the Hoogsteen base pair is a prerequisite for the opening of the Watson−Crick pair (pathway 2, Figure 6). However, if this is the case, and if the opening of the Hoogsteen and Watson−Crick base pairs are separate processes, we then would expect the opening of the Watson−Crick base pairs in the triplex system to have an apparent dissociation constant of the order 10^{-12} ($10^{-6} \times 10^{-6}$ from Table 1). Since it is only 10^{-7}, the most straightforward explanation is that Watson−Crick pairs open from within the closed base triplet (pathway 1, Figure 6).

It is worth noting that the stabilizing effect of the third strand in DNA-1 on the WC base pairs is approximately the same for a T·A−T and a G·G−C base triplet (WC5 and WC6, respectively). This is somewhat surprising since in the T·A−T base triplet the imino proton in the Watson−Crick pair is located on the thymine, which has only one H-bonding partner, whereas in the G·G−C triplet the corresponding imino proton is located on the central guanine, which is H-bonded by two partners. Hence, we would expect the central guanine to be much more restricted by the third strand than the flanking thymine. The observation suggests that the whole Watson−Crick base pair may behave like one unit regarding the exchange of its imino proton.

In conclusion, this study has given us a detailed picture of the base-triplet dynamics in a nature-like DNA triplex structure as well as a comparison with the corresponding duplex. The individual opening of the reverse Hoogsteen H-bonds follows the same principle as the opening of the WC H-bonds in a DNA duplex.

REFERENCES

1. Guéron, M., and Leroy, J.-L. (1992) Base-Pair Opening in Double-Stranded Nucleic Acids. *Nucleic Acids and Molecular Biology* (Eckstein, F., Lilley, D. M. J., Eds.) 1−22, Springer-Verlag, Berlin, Heidelberg.
2. Leroy, J. L., Charretier, E., Kochoyan, M., and Guéron, M. (1988) *Biochemistry 27*, 8894−8898.
3. Soyfer, V. N., and Potaman, V. N. (1996) *Triple-Helical Nucleic Acids*, Springer-Verlag, New York.
4. Mirkin, S., M., and Frank-Kamenetskii, M. D. (1994) *Annu. Rev. Biophys. Biomol. Struct. 23*, 541−576.
5. Praseuth, D., Guieysse, A. L., and Hélène, C. (1999) *Biochim. Biophys. Acta. 1489*, 181−206.
6. Wang, E., and Feigon, J. (1999) Structures of nucleic acid triplexes, in *Oxford Handbook of Nucleic Acid Structure* (Neidle, S., Ed.) 355−388, Oxford University Press, Oxford.
7. Cain, R. J., and Glick, G. D. (1998) *Biochemistry 37*, 1456−1464.
8. Powell, S. W., Jiang, L., and Russu, I. M. (2001) *Biochemistry 40*, 11065−11072.
9. Plateau, P., and Guéron, M. (1982) *J. Am. Chem. Soc. 104*, 7310−7311.
10. Guéron, M., Kochoyan, M., and Leroy, J. L. (1987) *Nature 328*, 89−92.
11. Geen, H., and Freeman, R. (1991) *J. Magn. Reson. 93*, 93−141.
12. Bauer, C., Freman, R., Frenkiel, T., Keeler, J., and Shaka, A. J. (1984) *J. Magn. Reson. 58*, 442−457.
13. Snoussi, K., and Leroy, J.-L. (2002) *Biochemistry 41*, 12467−12474.
14. Wärmländer, S., Sen, A., and Leijon, M. (2000) *Biochemistry 39*, 607−615.
15. Englander, S. W., and Kallenbach, N. R. (1983) *Q. Rev. Biophys. 16*, 521−655.
16. Eigen, M. (1964) *Angew. Chem. Intl. Ed. Engl. 3*, 1−72.
17. Forsén, S., and Hoffman, R. A. (1963) *Acta Chem. Scand. 17*, 1787−1788.
18. Radhakrishnan, I., de los Santos, C., and Patel, D. J. (1991) *J. Mol. Biol. 221*, 1403−1418.
19. Wüthrich, K. (1986) *NMR of Proteins and Nucleic Acids*, John Wiley & Sons, New York.
20. Pilch, D. S., Levenson, C., and Shafer, R. H. (1991) *Biochemistry 30*, 6081−6088.
21. Scaria, P. V., and Shafer, R. H. (1996) *Biochemistry 35*, 10985−10994.

BI034479U